

Supporting information

Ultra-stable and environmentally friendly CsPbBr₃@ZrO₂/PS composite films for white light-emitting diodes

Jindou Shi¹, Minqiang Wang*¹, Hao Wang¹, Chen Zhang¹, Yongqiang Ji¹, Junnan Wang¹, Yun
Zhou¹, Arshad Saleem Bhatti²

¹Electronic Materials Research Laboratory, Key Laboratory of the Ministry of Education
International Center for Dielectric Research&Shannxi Engineering Research Center of Advanced
Energy Materials and Devices, Xi'an Jiaotong University, 710049 Xi'an, China.

²Centre for Micro and Nano Devices, Department of Physics, COMSATS Institute of Information
Technology, Islamabad, 44500, Pakistan

Corresponding Author: E-mail: mqwang@xjtu.edu.cn

Supplementary Note 1

Experimental Section

1.1. Materials

The cesium carbonate (Cs_2CO_3 , 99.99%), oleic acid (OA, 85%), oleylamine (OAm, 80-90%), tri-n-octylphosphine (TOP, 90%), 1-octadecene (ODE, 90%), lead(II) bromide (PbBr_2 , 99.99%), zirconium butoxide solution ($\text{Zr}(\text{OC}_4\text{H}_9)_4$, 80%) were purchased from Aladdin. The poly(styrene) (PS) and toluene purchased from Shanghai Xianding Biological Technology Co Ltd and Shanghai Chemical Industrial Company. All the reagents were used without further purification.

1.2. Preparation of CsPbBr_3 QDs

Firstly, Cs-oleate solution was obtained by dissolving 0.4 g Cs_2CO_3 in a mixture of ODE (15 mL), OA (1.25 mL) and TOP (2 mL), followed by heating to 120°C under N_2 atmosphere until complete reaction. Subsequently, 138 mg of PbBr_2 was added to a mixture of ODE (10 mL), OA (1 mL) and OAm (1 mL), and heated to 170°C under a N_2 atmosphere until PbBr_2 was completely dissolved. Finally, 0.8 mL of Cs-oleate solution was rapidly injected into PbBr_2 solution at 170°C. After 5 s of reaction, the product was rapidly cooled to room temperature in an ice water bath and dispersed in toluene for storage.

1.3. Preparation of $\text{CsPbBr}_3@ZrO_2$ NCs.

Different amounts (0.0, 0.5, 1.0, 1.5, 2.0, 2.5 mL) of $\text{Zr}(\text{OC}_4\text{H}_9)_4$ dissolved in 10 mL of toluene was slowly added to the above CsPbBr_3 QDs toluene solution during stirring. The slow hydrolysis of $\text{Zr}(\text{OC}_4\text{H}_9)_4$ was carried out by stirring the solution for 10 h at room temperature and 80% relative humidity, followed by transferring the solution to a Teflon-lined stainless steel autoclave and then reacted at 170°C for 8 h. At the end of the reaction, the resulting product was collected by

centrifugation and dispersed with toluene.

1.4. Preparation of CsPbBr₃/PS CFs and CsPbBr₃@ZrO₂/PS CFs.

0.5 g of PS was dissolved in 4 mL of toluene and stirred at 60°C until completely dissolved, followed by cooling to room temperature with stirring. 1 mL of CsPbBr₃ QDs and CsPbBr₃@ZrO₂ NCs toluene solutions were added separately to the PS and stirred for 3 h until well mixed. Subsequently, the precursor solution was scraped onto the plate glass using blade coater and dried overnight at room temperature to obtain CsPbBr₃/PS CFs and CsPbBr₃@ZrO₂/PS CFs. CsPbCl₃@ZrO₂/PS CFs and CsPbI₃@ZrO₂/PS CFs were prepared in the same method as CsPbBr₃@ZrO₂/PS CFs, only the core layers were replaced with CsPbCl₃ and CsPbI₃.

1.5. White LED device assembled by CsPbBr₃/PS CFs and CsPbBr₃@ZrO₂/PS CFs.

As we all know, white light is composed of three basic colors (red, green and blue). In this article, the red light comes from CaSrAlN₃:Eu²⁺ (CSAN:Eu²⁺) phosphors, the green light was output from CsPbBr₃ QDs and CsPbBr₃@ZrO₂ NCs respectively, and the blue light is provided by a 450nm InGaN chip purchased by Shenzhen Xin Kai photoelectric Co Ltd. By optimization different amounts of CsPbBr₃ QDs or CsPbBr₃@ZrO₂ NCs and CSAN:Eu²⁺ phosphors are mixed and dispersed uniformly into toluene-dissolved PS and subsequently coated onto the surface of the InGaN chip. After drying at room temperature overnight, white LED devices are obtained.

Supplementary Note 2

Characterization Methods

The morphology and microstructure of CsPbBr₃ QDs or CsPbBr₃@ZrO₂ NCs were analyzed using a high-resolution TEM (JEOL JEM-F200) and EDS detector (Oxford X-Max 65) attached to a transmission electron microscope was utilized to study the chemical compositions of the sample.

The photoluminescence (PL) spectra, PL quantum yields (PLQYs) and time-resolved PL (TRPL) decay curves were recorded on an Edinburgh Instruments FLS 1000 spectrometer. The ultraviolet-visible (UV-Vis) absorption spectra were recorded by PE Lambda 950. The X-ray diffraction (XRD) patterns were obtained using the DB-ADVANCE X-ray diffraction analyzer diffractometer. X-ray photoelectron spectroscopy (XPS) spectra were measured by a Thermo Fisher ESCALA670B Xi⁺. The PL spectra of the samples at different temperatures were collected by Photo Research 670 spectrometer after heating the samples using a heater (MS7-H550-S, DLAB, China) and under 365 nm UV light irradiation. The electroluminance spectra of WLEDs were collected by a Keithley 2400 sourcemeter and a Photo Research 670 spectrometer.

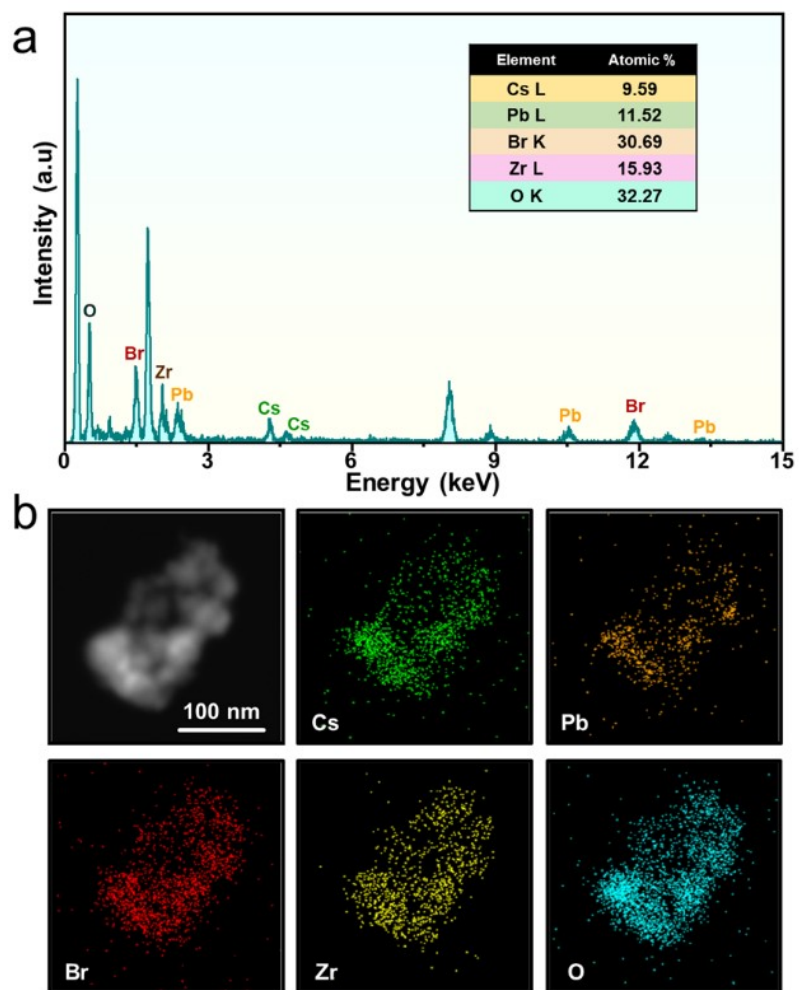


Fig. S1 The EDS mapping and spectrum (b) of CsPbBr₃@ZrO₂-0.5 NCs.

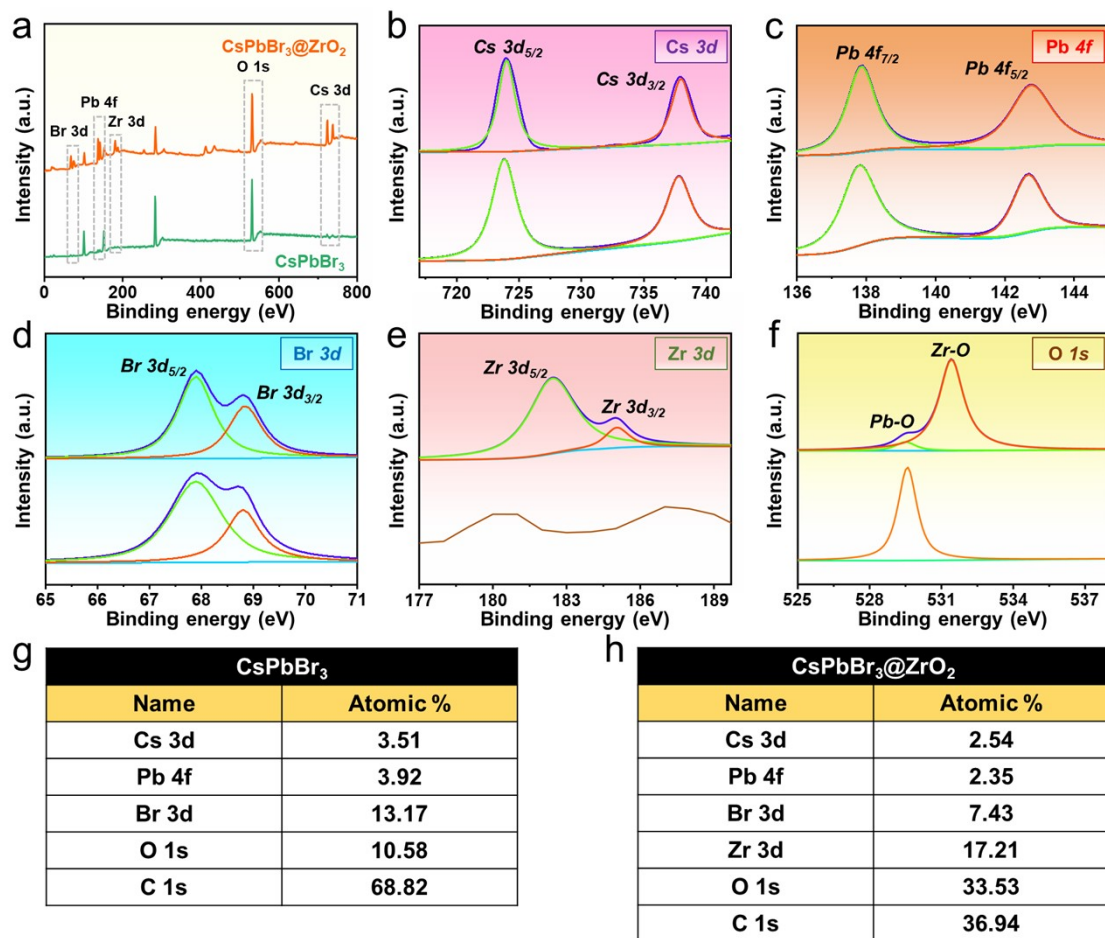


Fig. S2 XPS spectra of CsPbBr₃ QDs and CsPbBr₃@ZrO_{2-0.5} NCs: (a) Survey spectra, high-resolution signals of (b) Cs 3d, (c) Pb 4f, (d) Br 3d, (e) Zr 3d and (f) O 1s. The elemental ratios of (g) CsPbBr₃ QDs and (h) CsPbBr₃@ZrO_{2-0.5} NCs based on XPS measurements.

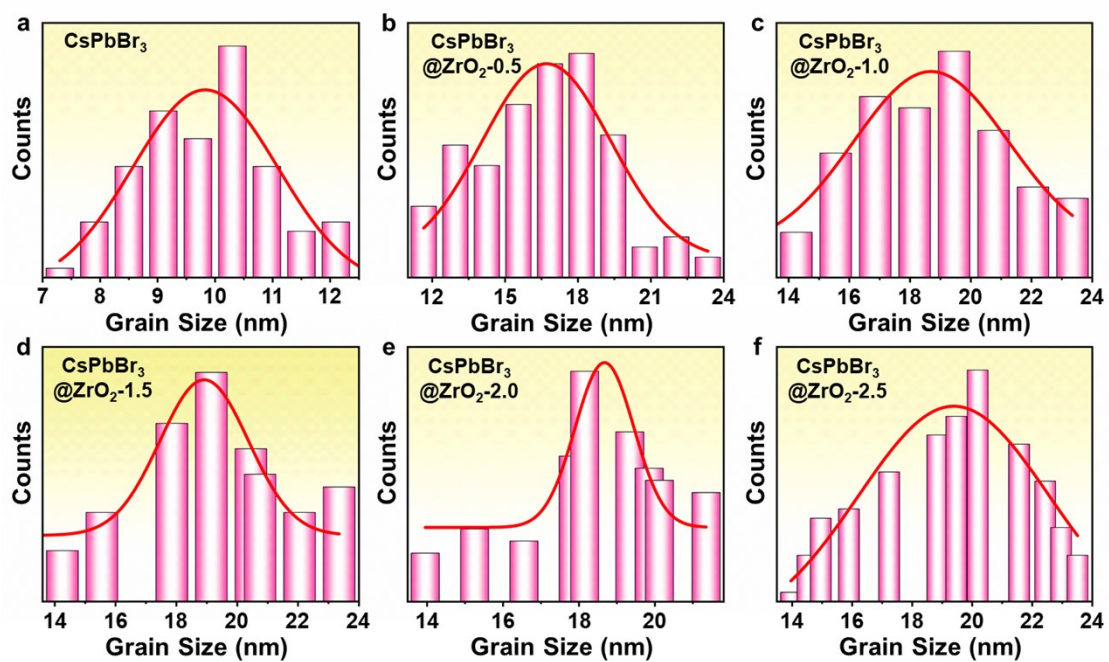


Fig. S3 Grain size of samples prepared with different amounts (0.0, 0.5, 1.0, 1.5, 2.0, 2.5 mL) of

$\text{Zr}(\text{OC}_4\text{H}_9)_4$.

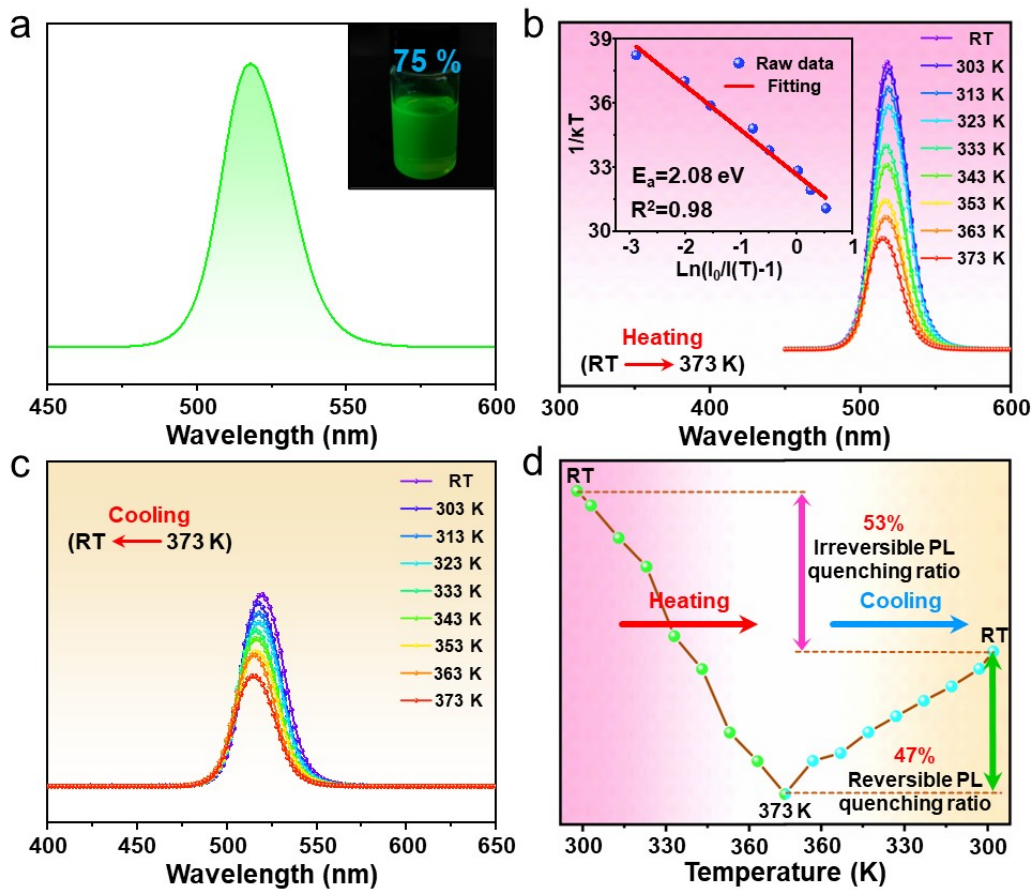


Fig. S4 PL spectrum of CsPbBr₃@ZrO₂ -2.0 NCs before the solvothermal reaction. PL spectra of CsPbBr₃@ZrO₂ -2.0 NCs during heating (b) and cooling (c) cycles at 373 K, corresponding to the analysis (d) of the relative change in PL intensity. Inset in (a) is a photograph of CsPbBr₃@ZrO₂ -2.0 NCs before the solvothermal reaction under 365 nm UV light and its corresponding PLQY value. Inset in (b) is the relationship between $\ln(I_0/I(T)-1)$ versus $1/\kappa T$ for CsPbBr₃ QDs and CsPbBr₃@ZrO₂ NCs.

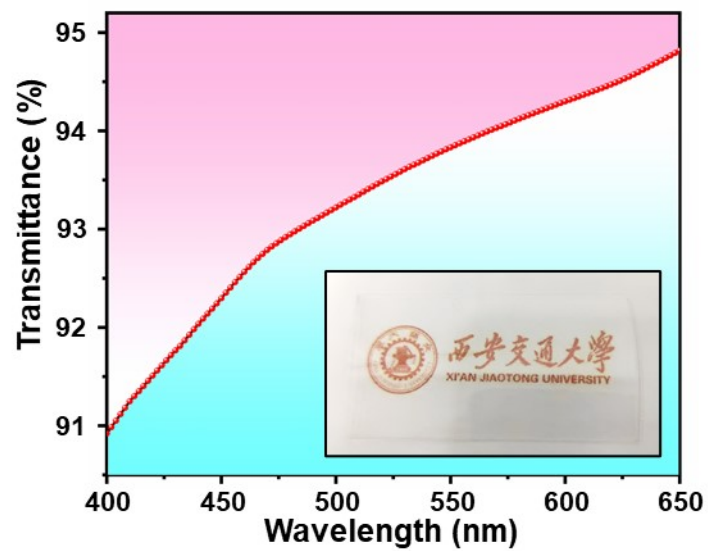


Fig. S5 Optical transmission spectrum of a pure PS film, inset shows the optical transmittance photograph of the corresponding film.

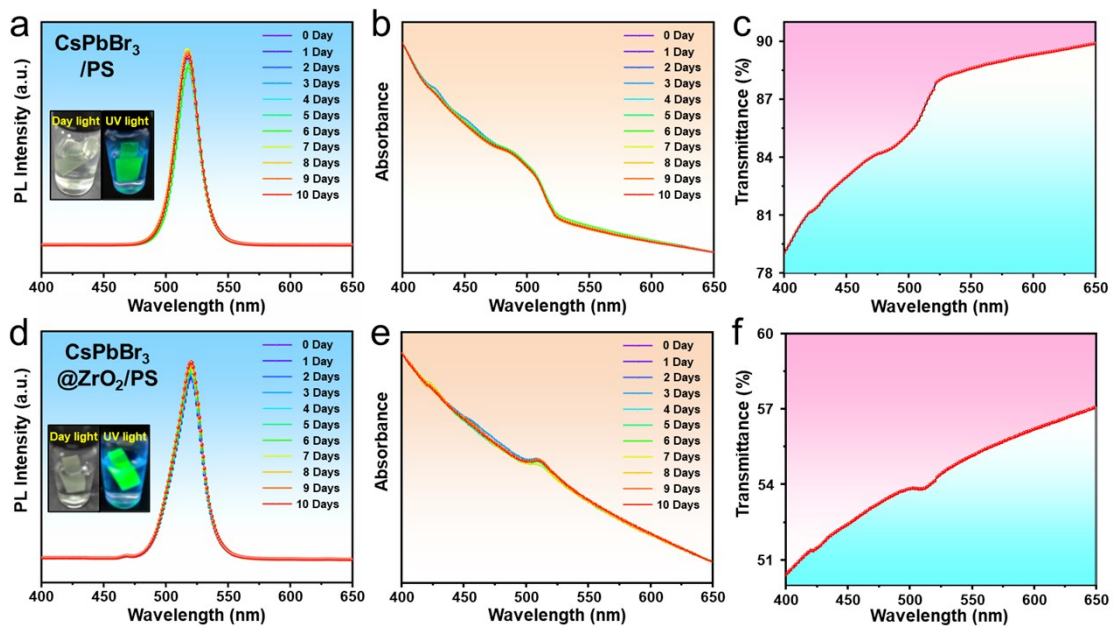


Fig. S6 Optical transmission spectrum of a pure PS film, inset shows the optical transmittance photograph of the corresponding film.

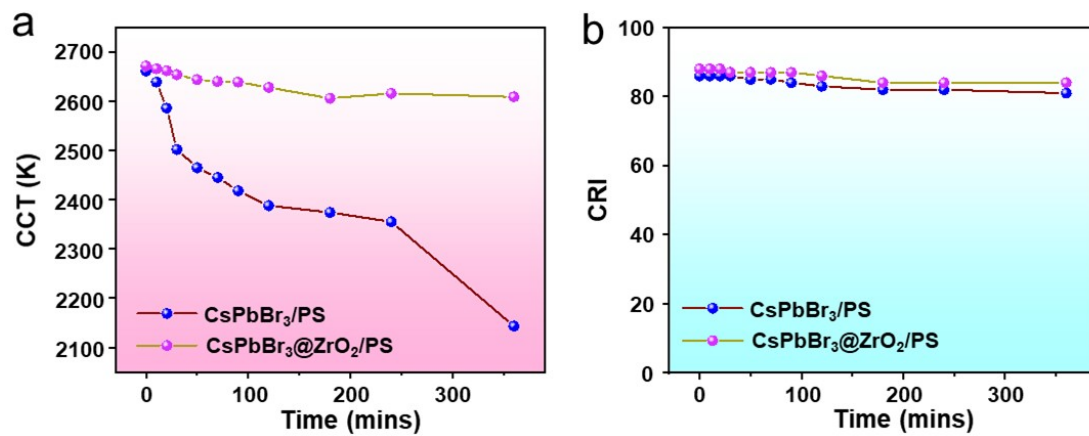


Fig. S7 Changes in CCT (a) and CRI (b) for two WLEDs at different operating times.

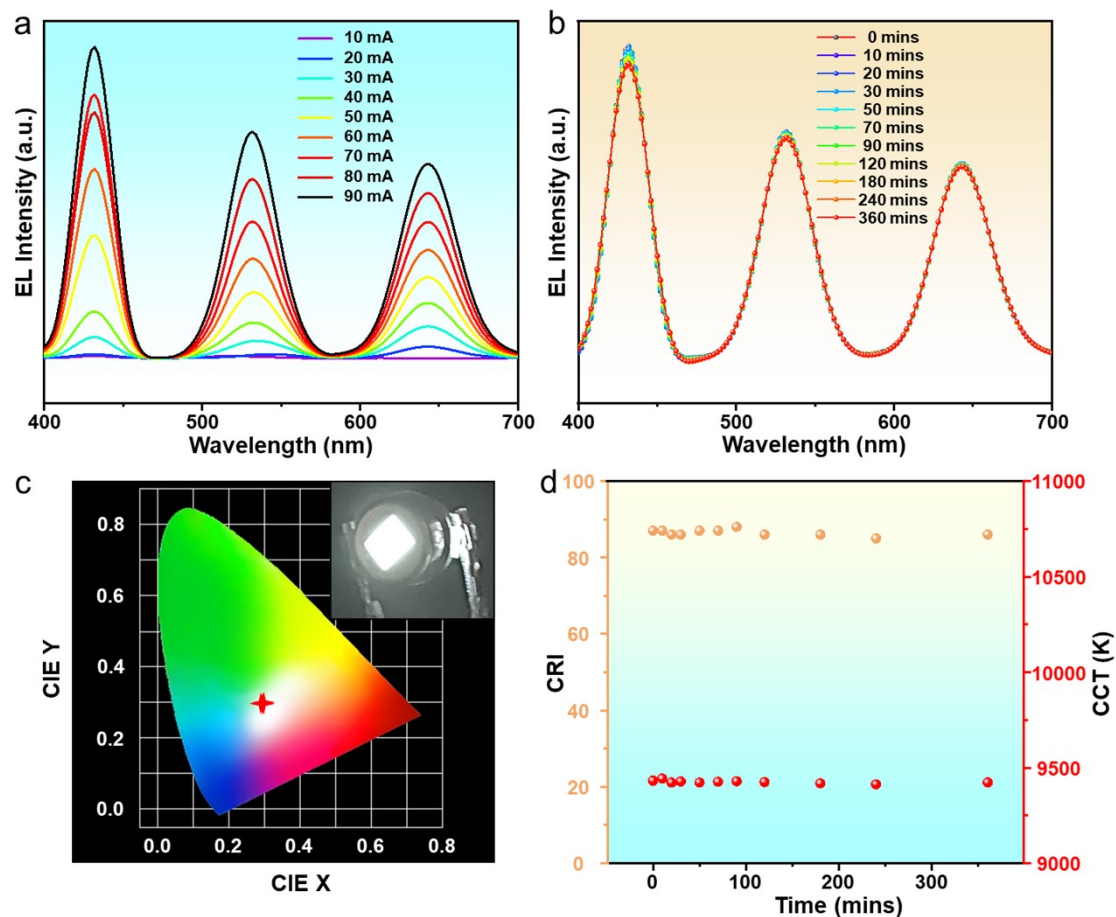


Fig. S8 EL spectra (a) of WLED assembled with $\text{CsPbCl}_3@ZrO_2$, $\text{CsPbBr}_3@ZrO_2$ and $\text{CsPbI}_3@ZrO_2$ at different drive currents. Changes in the EL spectra (b), CIE color coordinates (c), CRI (yellow) and CCT (red) (d) of WLED device driven by 90 mA current with extended operating time. The inset in (c) is photograph of the corresponding WLED in operation.

Table. S1 Bi-exponential fitting results of PL decays for samples prepared with different amounts (0.0,

Zr(OC ₄ H ₉) ₄ (mL)	τ_1 (ns)	A ₁ (%)	τ_2 (ns)	A ₂ (%)	τ_{ave} (ns)
0.0	2.9241	13.72	13.6469	86.28	13.2936
0.5	2.7911	6.72	18.7303	93.28	18.561
1.0	3.5182	4.17	20.3413	95.83	20.2156
1.5	5.2508	3.92	23.6848	96.08	23.5196
2.0	2.7905	4.54	24.7902	95.46	24.6731
2.5	3.1815	6.75	21.5706	93.25	21.3763

0.5, 1.0, 1.5, 2.0, 2.5 mL) of Zr(OC₄H₉)₄.

The PL decay curves of different samples were studied and the decay traces for the samples were well fitted with bi-exponential decay function $Y(t)$ based on nonlinear least-squares, using the following expression.

$$Y(t) = A_1 \exp\left(-\frac{t}{\tau_1}\right) + A_2 \exp\left(-\frac{t}{\tau_2}\right) \quad (S1)$$

where A_1, A_2 are fractional contributions of time-resolved emission decay lifetimes τ_1, τ_2 .

The average lifetime (τ_{ave}) of the different samples can be obtained by the following equation.

$$\tau_{ave} = \frac{A_1 \tau_1^2 + A_2 \tau_2^2}{A_1 \tau_1 + A_2 \tau_2} \quad (S2)$$

Thermoplastics polystyrene (PS)^{1, 2}, polyethylene (PE)³⁻⁵, polypropylene (PP)^{6, 7} and polymethyl methacrylate (PMMA)⁸⁻¹⁰ have been reported to be used for surface encapsulation of optoelectronic devices due to their high light transmission¹¹⁻¹³. However, cesium lead halide perovskite CsPbBr₃ (X=Cl, Br, I) materials are often used in practical applications due to the overheating of the device will reduce its optical characteristics. Therefore, thermoplastics with higher thermal stability will be the first choice for encapsulation of perovskite optoelectronic devices^{14, 15}.

As a thermoplastic, PS has excellent mechanical properties such as high strength, superior toughness, wear resistance, and aging resistance and so on¹⁶. At the same time, it has high transparency¹³, high waterproof¹⁷, windproof, antibacterial¹⁸, mudproof, heat preservation, anti-ultraviolet radiation, and can still maintain a certain degree of flexibility at room temperatures¹⁹. More importantly, its good thermal insulation properties will promote the wide application of perovskite in optoelectronic devices²⁰.

Table S2 Comparison of PS and traditional thermoplastic polymer encapsulation materials

Properties indexes	Thermoplastic plastics			
	PS	PE	PP	PMMA
Light transmittance	92%	90%	60%	92%
Decomposition temperature	250°C	220°C	200°C	150°C
Thermal resistance	+	+	0	-
Impact resistance	+	-	+	0
Surface hardness	+	-	+	0
Ageing resistance	+	-	0	+
Water resistance	+	+	+	+

Tenacity

+

+

0

0

Note: +, 0, -, represent excellent, better, and poor, respectively.

Reference

- 1 X. T. Yang and Y. Zhang, *Langmuir*, 2004, **20**, 6071-6073.
- 2 Y. Wei, X. R. Deng, Z. X. Xie, X. C. Cai, S. S. Liang, P. Ma, Z. Y. Hou, Z. Y. Cheng and J. Lin, *Adv Funct Mater*, 2017, **27**, 1703535.
- 3 K. Suizu and N. Harada, *Int Arch Occ Env Hea*, 2005, **78**, 311-318.
- 4 M. Erdmann, A. Kupsch, B. R. Muller, M. P. Hentschel, U. Niebergall, M. Bohning and G. Bruno, *J Mater Sci*, 2019, **54**, 11739-11755.
- 5 P. D. Kalb, P. R. Lageraen and S. Wright, *J Environ Sci Heal A*, 1996, **31**, 1767-1780.
- 6 A. Rout, P. Pandey, E. F. Oliveira, P. A. D. Autreto, A. Gumaste, A. Singh, D. S. Galvao, A. Arora and C. S. Tiwary, *Polymer*, 2019, **169**, 148-153.
- 7 B. Wen, F. Wang, X. F. Xu, Y. F. Ding, S. M. Zhang and M. S. Yang, *Polym-Plast Technol*, 2011, **50**, 1375-1382.
- 8 U. Ali, K. J. B. Abd Karim and N. A. Buang, *Polym Rev*, 2015, **55**, 678-705.
- 9 F. Ahangaran, A. H. Navarchian and F. Picchioni, *J Appl Polym Sci*, 2019, **136**, 48039.
- 10 A. Sari, C. Alkan and C. Bilgin, *Appl Energ*, 2014, **136**, 217-227.
- 11 I. V. Pollet and J. G. Pieters, *J Agr Eng Res*, 2000, **75**, 65-72.
- 12 S. M. Lai, W. C. Chen and X. S. Zhu, *Compos Part a-Appl S*, 2009, **40**, 754-765.
- 13 H. Li, J. F. Wang, S. L. Li, J. Robichaud, D. Wang, Z. Wu and Y. Djaoued, *J Mater Chem C*, 2019, **7**, 2978-2986.

- 14 J. D. Peterson, S. Vyazovkin and C. A. Wight, *Macromol Chem Physic*, 2001, **202**, 775-784.
- 15 M. Ferriol, A. Gentilhomme, M. Cochez, N. Oget and J. L. Mieloszynski, *Polym Degrad Stabil*, 2003, **79**, 271-281.
- 16 R. B. Mathur, S. Pande, B. P. Singh and T. L. Dhami, *Polym Composite*, 2008, **29**, 717-727.
- 17 Y. F. Lin, W. W. Wang and C. Y. Chang, *J Mater Chem A*, 2018, **6**, 9489-9497.
- 18 A. M. Youssef, S. Kamel and M. A. El-Samahy, *Carbohydr Polym*, 2013, **98**, 1166-1172.
- 19 H. F. Fei, B. M. Yayitt, X. Y. Hu, G. Kopanati, A. Ribbe and J. J. Watkins, *Macromolecules*, 2019, **52**, 6449-6457.
- 20 M. Khoukhi, N. Fezzioui, B. Draoui and L. Salah, *Appl Therm Eng*, 2016, **105**, 669-674.